Mon. Not. R. Astron. Soc. **262,** 1007–1012 (1993)

A perturbation particle method for stability studies of stellar systems

Felipe C. Wachlin,[1] George B. Rybicki[2] and Juan C. Muzzio[1]

[1] *Facultad de Ciencias Astronómicas y Geofísicas de la Universidad Nacional de La Plata and Programa de Fotometría y Estructura Galáctica del Consejo Nacional de Investigaciones Científicas y Técnicas de la República Argentina, Paseo del Bosque, 1900 La Plata, Argentina*

[2] *Harvard–Smithsonian Center for Astrophysics, 60 Garden Street, Cambridge, MA 02138, USA*

Accepted 1992 December 18. Received 1992 November 11

ABSTRACT

We discuss a numerical method for investigating the stability of stellar systems that uses an analytic distribution function to describe a stellar system in equilibrium and 'perturbation particles' to represent departures from that equilibrium state. The particles are used only to represent the perturbation, and statistical fluctuations due to the finite number of particles are therefore much less severe than in full N-body codes. We provide a general description of the method, recipes for particular aspects of its implementation, and an example of its application to a simple model with known analytical solution.

Key words: instabilities – methods: numerical – celestial mechanics, stellar dynamics.

1 INTRODUCTION

The analytical investigation of the stability of stellar systems is often limited by the complexity of the mathematics involved (see, e.g., the excellent chapter on the subject in the textbook by Binney & Tremaine 1987), and so numerical methods are frequently needed (see e.g. Merritt & Aguilar 1985). Nevertheless, the necessarily finite number of particles used in N-body simulations causes statistical fluctuations that affect the results, not only by merely limiting their precision but also, more subtly, by causing a time-dependent potential that produces random changes in the energy of individual particles (Hernquist & Ostriker 1992). While these difficulties may be the unavoidable price to pay in problems that demand the use of a full N-body code, they seem to impose an excessive tax on stability analyses, where interest is centred on the (usually small) perturbation and not on the basic system that is perturbed. Worst of all, a small perturbation might even completely disappear in the noise caused by the random fluctuations. If it were possible, instead, to use particles to represent *only* the perturbation, we would end up with statistical fluctuations in the perturbation itself that would be much less problematic.

It is therefore not surprising that several researchers have investigated methods that use particles to represent just a perturbation, and not the whole perturbed system (Merritt 1992, private communication). Although the basic ideas are simple enough, the practical implementation of these methods presents some difficulties, which may help to explain why so little has been published on this subject: to our knowledge, there is only a brief description presented by Merritt (1987), within a paper on a more general subject.

We have therefore decided to present here a detailed description of the perturbation particle method (Section 2), followed by its application to a particularly simple system whose theoretical solution is known (Sections 3 and 4); we emphasize some practical aspects of the method, such as the need to sample the whole phase space and how to choose the phase-space volumes for each particle. Finally, Section 5 discusses our results.

2 THE METHOD

Let us consider a self-gravitating stellar system; at any point in phase space, defined by the position and velocity vectors $\boldsymbol{x}$ and $\boldsymbol{v}$ respectively, and at any time t, the mass density in (six-dimensional) phase space is given by the distribution function $f(\boldsymbol{x}, \boldsymbol{v}, t)$. If the number of stars in the system is large enough, the effect of the individual stellar encounters can be neglected and the system obeys the collisionless Boltzmann equation:

$$\frac{\partial f}{\partial t}+\boldsymbol{v}\cdot\frac{\partial f}{\partial \boldsymbol{x}}-\frac{\partial \Phi}{\partial \boldsymbol{x}}\cdot\frac{\partial f}{\partial \boldsymbol{v}}=0, \tag{1}$$

where $\Phi(\boldsymbol{x}, t)$ is the gravitational potential created by the stellar system itself. The Boltzmann equation simply states that the phase-space mass density remains constant along the trajectory of any particle in phase space.

Let us assume now that the state of the stellar system characterized by $f(\boldsymbol{x}, \boldsymbol{v}, t)$ and $\Phi(\boldsymbol{x}, t)$ is the result of the perturbation [with a perturbation represented by a mass phase-space density $f_1(\boldsymbol{x}, \boldsymbol{v}, t)$ and a potential $\Phi_1(\boldsymbol{x}, t)$] of an equilibrium state characterized by a mass phase-space den-

sity $f_0(\boldsymbol{x}, \boldsymbol{v})$ and a potential $\Phi_0(\boldsymbol{x})$. Since f_0 and Φ_0 also obey equation (1), and since $f = f_0 + f_1$ and $\Phi = \Phi_0 + \Phi_1$, it is easy to show that

$$\frac{\partial f_1}{\partial t} + \boldsymbol{v} \cdot \frac{\partial f_1}{\partial \boldsymbol{x}} - \frac{\partial \Phi}{\partial \boldsymbol{x}} \cdot \frac{\partial f_1}{\partial \boldsymbol{v}} = \frac{\partial \Phi_1}{\partial \boldsymbol{x}} \cdot \frac{\partial f_0}{\partial \boldsymbol{v}} . \tag{2}$$

If we assume that the perturbation is small, i.e. that $|\Phi_0| \gg |\Phi_1|$ and $f_0 \gg f_1$, equation (2) can be linearized, replacing the term $\partial\Phi/\partial\boldsymbol{x}$ by $\partial\Phi_0/\partial\boldsymbol{x}$, because the product $(\partial\Phi_1/\partial\boldsymbol{x})\cdot(\partial f_1/\partial\boldsymbol{v})$ is of second order in the perturbation:

$$\frac{\partial f_1}{\partial t} + \boldsymbol{v} \cdot \frac{\partial f_1}{\partial \boldsymbol{x}} - \frac{\partial \Phi_0}{\partial \boldsymbol{x}} \cdot \frac{\partial f_1}{\partial \boldsymbol{v}} = \frac{\partial \Phi_1}{\partial \boldsymbol{x}} \cdot \frac{\partial f_0}{\partial \boldsymbol{v}} . \tag{3}$$

We may write either of equations (2) and (3) as

$$\left(\frac{\mathrm{D}f_1}{\mathrm{D}t} \right)_{\mathrm{traj}} = \frac{\partial \Phi_1}{\partial \boldsymbol{x}} \cdot \frac{\partial f_0}{\partial \boldsymbol{v}} , \tag{4}$$

where $(\mathrm{D}/\mathrm{D}t)$ denotes the convective or Lagrangian derivative along the trajectory of a particle in phase space: if the trajectory is that followed in the total potential Φ, we obtain equation (2); if, instead, the trajectory is that followed in the unperturbed potential Φ_0, we obtain equation (3). In any case, equation (4) gives the change in f_1 as we proceed along the trajectory in question.

It is at this point that we may introduce an N-body approach to solve equation (4). The form of the equation suggests that we might use fictitious, or perturbation, particles to represent f_1. The particles would follow the corresponding trajectories, either in Φ or in Φ_0, but they would have variable masses, so that their mass changes accounted for the changes in f_1. We must, of course, accept the possibility of negative masses, since f_1 can take negative values. The conversion from f_1 to perturbation particles, and vice versa, requires a phase-space volume Γ_i to be defined for each particle of mass m_i; according to Liouville's theorem, these volumes can be taken as constant as the system evolves. Thus we may write

$$\frac{\mathrm{D}f_1(\boldsymbol{x}_i, \boldsymbol{v}_i, t)}{\mathrm{D}t} = \frac{\dot{m}_i}{\Gamma_i} , \tag{5}$$

and, comparing with equation (4), we obtain an equation for $\dot{m}_i$:

$$\dot{m}_i = \Gamma_i \cdot \frac{\partial \Phi_1}{\partial \boldsymbol{x}_i} \cdot \frac{\partial f_0}{\partial \boldsymbol{v}_i} . \tag{6}$$

Usually, the particle–particle interaction will be accounted for by a softened Newtonian potential (an example that uses a different law is given in Sections 3 and 4), so that the equations to be solved numerically are

$$\dot{\boldsymbol{x}}_i = \boldsymbol{v}_i , \tag{7}$$

$$\dot{\boldsymbol{v}}_i = -\frac{\partial \Phi_0(\boldsymbol{x}_i)}{\partial \boldsymbol{x}_i} - G \sum_{j=1}^{N} \frac{m_j(\boldsymbol{x}_i - \boldsymbol{x}_j)}{[\varepsilon^2 + (\boldsymbol{x}_i - \boldsymbol{x}_j)^2]^{3/2}} , \tag{8}$$

$$\dot{m}_i = \Gamma_i \frac{\partial f_0(\boldsymbol{x}_i, \boldsymbol{v}_i)}{\partial \boldsymbol{v}_i} \cdot G \sum_{j=1}^{N} \frac{m_j(\boldsymbol{x}_i - \boldsymbol{x}_j)}{[\varepsilon^2 + (\boldsymbol{x}_i - \boldsymbol{x}_j)^2]^{3/2}} . \tag{9}$$

Equations (7) and (9) are the same for both the exact and linearized approaches. As it stands, equation (8) corresponds to the exact solution; to obtain the linearized version, one only has to omit the summation over j.

Some care should, however, be exercised when implementing the perturbation particle method. For example, the first idea that comes to mind is to create (say, using a pseudo-random number generator) a distribution of perturbation particles that reproduces the initial perturbation, $f_1(\boldsymbol{x}, \boldsymbol{v}, 0)$, and then follow its time evolution using equations (7)–(9). A little reflection shows, however, that we will err badly if we place perturbation particles only at the location of the initial perturbation: the perturbation particles are the only means we have to check the response of the system, so they must be present from the very beginning in every region of the phase space occupied not only by the perturbation, but by the whole system (i.e. where f_0 differs significantly from zero). For example, let us consider a spherical stellar system in equilibrium, and let us add a perturbation in the form of an excess mass in a spherical shell concentric with the system. All the particles located outside the shell will immediately feel a force stronger than that due to the original system, and their distribution will also be immediately affected. The subsequent changes in these outer regions will, however, be impossible to detect, unless we have placed perturbation particles there too, and not only in the shell. In brief, we can mimic the initial perturbation using positive and negative mass perturbation particles, but we must also cover the rest of the phase space occupied by the system with zero-mass perturbation particles; as the system evolves, these zero masses might become positive or negative, reflecting the changes caused in the regions in which there was initially no perturbation by the perturbed gravitational fields from other regions.

There does not seem to be a self-evident, unique way to choose the phase-space volumes to be assigned to each particle. It is therefore important to check the robustness of the method in this respect. In Section 4 we propose two reasonable, although not compelling, ways to select these volumes, and we show that the results of our examples are not much affected by this selection.

Finally, since the total mass of the perturbation must be conserved, the sum of the masses of the perturbation particles must remain constant throughout the integration. This condition provides a check on the accuracy of the numerical computation, just as the conservation of energy provides a check for the regular N-body simulations.

3 A SIMPLE THEORETICAL MODEL

The first check of the perturbation particle method that comes to mind is the simple case of a plane wave propagating in an infinite homogeneous medium. This case gives rise to the well-known Jeans instability (e.g. Binney & Tremaine 1987), but, on second thoughts, some difficulties appear. One of these is that a Newtonian force law must be softened for numerical experiments, in order to avoid singularities in the equations of motion; this might complicate the comparison of theoretical and numerical results. Another difficulty is that the results for the Jeans instability pertain to a three-dimensional space, and a problem that is just one-dimensional would be simpler to check.

Fortunately, we have found a one-dimensional case that needs no additional softening and yields results very similar to those of the Jeans instability. Let us consider an infinite linear distribution of particles along the x-axis, and let us call the velocity along this axis u, so that the distribution function of the particles at time t is $f(x, u, t)$, and the linear mass density of the distribution is therefore

$$\lambda(x, t)=\int_{-\infty}^{\infty} f(x, u, t)\,\mathrm{d}u. \tag{10}$$

Let us also assume that the force law is such that the acceleration it exerts on one of its particles, at the position x', is

$$a(x')=\mu\int_{-\infty}^{\infty}\lambda(x, t)\,\mathrm{sgn}(x-x')\exp(-\nu|x-x'|)\,\mathrm{d}x, \tag{11}$$

where μ and ν are constants related, respectively, to the strength and to the scalelength of the force field. This form is a generalization of the usual one-dimensional gravitating sheet result, to which it reduces when $\nu=0$. It is easy to see that if the system is homogeneous, i.e. if $\lambda(x, t)=\lambda_0=$ constant, then the total acceleration on a particle is zero, as is verified directly by substitution into the integral in equation (11). Because this integral converges, the inconsistencies that plague the usual Newtonian case do not appear in this case, and one is not forced to use the 'Jeans swindle' (see e.g. Binney & Tremaine 1987).

Let us now consider an infinite homogeneous linear distribution, whose distribution function is $f_0(u)$, and a small perturbation $f_1(x, u, t)$, so that $f=f_0+f_1$. We can obtain f_1 using equation (3), taking into account that $(\partial\Phi_0/\partial x)=0$ and

$$\frac{\partial\Phi_1}{\partial x}=\mu\int_{-\infty}^{\infty}\lambda_1(x', t)\,\mathrm{sgn}(x-x')\exp(-\nu|x-x'|)\,\mathrm{d}x', \tag{12}$$

where λ_1 is the linear mass density of the perturbation, i.e. the integral of f_1 over all possible values of the velocity u.

If we adopt a Gaussian distribution of velocities for f_0,

$$f_0(u)=\frac{\lambda_0}{\sigma(2\pi)^{1/2}}\exp[-(u^2/2\sigma^2)], \tag{13}$$

and a wave form for f_1,

$$f_1(x, u, t)=f_a(u)\exp[\mathrm{i}(kx-\omega t)], \tag{14}$$

it is easy to follow the same mathematical formalism used to investigate the Jeans instability (see e.g. Binney & Tremaine 1987) to obtain the dispersion relation

$$1-\frac{2k\mu\lambda_0}{\sigma^3(k^2+\nu^2)(2\pi)^{1/2}}\int_{-\infty}^{\infty}\frac{\exp[-(u^2/2\sigma^2)]}{ku-\omega}u\,\mathrm{d}u=0, \tag{15}$$

which, calling k_J the wavenumber for $\omega=0$, where

$$k_\mathrm{J}^2=(2\mu\lambda_0/\sigma^2)-\nu^2, \tag{16}$$

we can write as

$$1-\frac{k_\mathrm{J}^2+\nu^2}{k^2+\nu^2}\frac{1}{\sigma(2\pi)^{1/2}}\int_{-\infty}^{\infty}\frac{\exp[-(u^2/2\sigma^2)]}{u-\omega/k}u\,\mathrm{d}u=0, \tag{17}$$

which is very similar to the dispersion relation for the Jeans instability, except that the quotient (k_J^2/k^2) is replaced here by the quotient $[(k_\mathrm{J}^2+\nu^2)/(k^2+\nu^2)]$. The results given by Binney & Tremaine (1987) can thus be easily adapted to the present case for $\omega=0$ (stationary wave), and for ω purely imaginary and positive (unstable solutions which can be evaluated in terms of the error function). When the imaginary part of ω is negative, we obtain damped solutions whose traditional analysis, following Landau's method, is much more difficult (see e.g. Binney & Tremaine 1987). Nevertheless, very recently, Maoz (1991) has shown that Landau damping is in fact irrelevant in stellar systems, and that the damping is essentially due to phase mixing. Following Maoz, we may assume that self-gravity can be neglected and consider only the reduced Boltzmann equation

$$\frac{\partial f_1}{\partial t}+u\frac{\partial f_1}{\partial x}=0, \tag{18}$$

whose general solution is, of course, $f_1(x-ut, u)$. Taking the initial perturbation as

$$f_1^0(x, u, 0)=\frac{\Lambda_1}{\sigma(2\pi)^{1/2}}\cos(kx)\exp[-(u^2/2\sigma^2)], \tag{19}$$

we can easily obtain the perturbation in the distribution function,

$$f_1^0(x, u, t)=\frac{\Lambda_1}{\sigma(2\pi)^{1/2}}\cos[k(x-ut)]\exp[-(u^2/2\sigma^2)], \tag{20}$$

and the perturbation in the linear mass density,

$$\lambda_1^0(x, t)=\Lambda_1\cos(kx)\exp[-(k\sigma t)^2/2]. \tag{21}$$

This is essentially Maoz's method, but we can now proceed one step further and obtain a better approximation that takes into account self-gravity (notice that we have used f_1^0 and λ_1^0 for f_1 and λ_1, respectively, to indicate that they are approximations of only zeroth order). From equations (12) and (21), we can easily compute a zeroth-order approximation for the force (with the sign changed):

$$\frac{\partial\Phi_1^0}{\partial x}=\frac{2\mu\Lambda_1 k}{k^2+\nu^2}\sin(kx)\exp[-(k\sigma t)^2/2], \tag{22}$$

and, using this approximation in the full linearized Boltzmann equation (3), we can obtain a first-order approximation for f_1:

$$\begin{aligned}f_1^1(x, u, t)=\frac{\Lambda_1}{\sigma(2\pi)^{1/2}}\Bigg\{&\cos[k(x-ut)]\exp[-(u^2/2\sigma^2)]\\&-\frac{2\mu\lambda_0 k}{\sigma^2(k^2+\nu^2)}u\exp[-(u^2/2\sigma^2)]\\&\times\int_0^t\exp[-(k\sigma\tau)^2/2]\sin\{k[x+u(\tau-t)]\}\,\mathrm{d}\tau\Bigg\}.\end{aligned} \tag{23}$$

To obtain a first-order approximation for the linear mass density, we only have to integrate over all possible values of the velocity, u:

$$\lambda_1^1(x,t)=\Lambda_1\cos(kx)\left\{\exp[-(k\sigma t)^2/2]+\frac{k_j^2+\nu^2}{k^2+\nu^2}\,k\sigma t\exp[-(k\sigma t)^2/4]\frac{\sqrt{\pi}}{2}\operatorname{erf}(k\sigma t/2)\right\}, \quad (24)$$

where $\operatorname{erf}(z)$ denotes the error function of z. This procedure can be iterated to obtain higher order approximations; the second-order approximation turns out to be

$$\lambda_1^2(x,t)=\Lambda_1\cos(kx)\left\{\exp[-(k\sigma t)^2/2]+\frac{k_j^2+\nu^2}{k^2+\nu^2}\,k\sigma t\exp[-(k\sigma t)^2/4]\frac{\sqrt{\pi}}{2}\operatorname{erf}(k\sigma t/2)-\left(\frac{k_j^2+\nu^2}{k^2+\nu^2}\right)^2\int_0^{k\sigma t}\tau(\tau-k\sigma t)\times\exp[-(\tau-k\sigma t)^2/2-\tau^2/4]\frac{\sqrt{\pi}}{2}\operatorname{erf}\left(\frac{\tau}{2}\right)d\tau\right\}. \quad (25)$$

Successive approximations add terms of the order of $[(k_j^2+\nu^2)/(k^2+\nu^2)]^i$, where i is the order of the approximation. Clearly, these additional terms become negligibly small for $k>k_j$, in good agreement with Maoz's (1991) conclusion that phase mixing is the most important cause of damping for $\lambda<\lambda_j$. For $\lambda=0.5\lambda_j$, which we will consider in one of the examples that follows, the relative part of the wave energy that dissipates due to Landau damping is less than 3 per cent (Maoz's equation 17 and table 1), so that the small correction provided by our second-order approximation is all we need for a comparison with the numerical results.

4 COMPARISON OF NUMERICAL AND THEORETICAL RESULTS

In order to use the simple model of Section 3 to test the perturbation particle method, we prepared a simple one-dimensional code with a Runge–Kutta integrator. Since, as we show here, the tests were successful, we are now preparing a three-dimensional code with a (much more efficient) polynomial integrator similar to that of the NBODY1 code of Aarseth (1985). The code was run in a 486 personal computer and in a Hewlett–Packard 9000 (Apollo) work station; the total number of perturbation particles was taken as $N=1000$ for all the cases considered.

In order to represent the infinite extension of the system, we imposed periodic boundary conditions and applied the numerical method to a one-wavelength region only. We adopted the following values for the different constants: $\mu=1$, $\nu=2$, $\lambda_0=1$ and $\sigma=0.214$, so that the Jeans wavelength is $\lambda_j=2\pi/k_j=1$. In what follows, cases a, b and c refer to experiments in which we adopted perturbation wavelengths equal to λ_j, $0.5\lambda_j$ and $1.25\lambda_j$, respectively; in other words, case a corresponds to a stationary wave, case b to a damped wave, and case c is unstable. In every case, the initial amplitude of the wave is such that the total (positive) mass excess is 0.025 and the corresponding total (negative) mass deficit is -0.025.

As indicated in Section 3, there is no unique way of choosing the phase-space volumes, Γ_i, that correspond to each of the perturbation particles of mass m_i. One way of doing so which may be reasonable seems to be to select the volumes in such a way that all the particles have initially the same mass, that is, to adopt volumes proportional to the inverse of the value of the *perturbation* in the distribution function at the initial position of the particle in question:

$$\Gamma_i\propto\frac{1}{f_1[\boldsymbol{x}_i(0),\boldsymbol{v}_i(0)]}. \quad (26)$$

Another possibly reasonable procedure seems to be to choose all the volumes equal, i.e.

$$\Gamma_i=\Gamma. \quad (27)$$

Although the mean value of the volumes is necessarily the same with the two procedures, the former results in a considerable dispersion of values around the mean, as shown in Table 1. The two procedures therefore offer fairly different values for the volumes and provide a useful test of the robustness of the method in this sense. It is worth emphasizing that, as the mass of a particle divided by the volume assigned to it must be equal to the perturbation in the distribution function, a different selection of volumes necessarily implies a different selection of masses.

Table 1. Statistics of the two volume choices.

	Γ_i choice	Case *a*	Case *b*	Case *c*
Mean Γ_i	1	0.0010700	0.0005350	0.0013375
Dispersion	1	0.0016219	0.0007939	0.0017682
Minimum Γ_i	1	0.0000064	0.0000064	0.0000161
Maximum Γ_i	1	0.0168311	0.0090051	0.0181017
Γ_i	2	0.0010700	0.0005350	0.0013375

In what follows, we indicate the experiments that use the first procedure with the number 1, and those that use the second with the number 2. That is, experiment 1b selects the volumes with equation (26) and deals with a perturbation of wavelength $0.5\lambda_j$, while experiment 2a uses equation (27) to investigate a perturbation of wavelength λ_j.

One complication arises from the fact that the velocity distributions of our model extend to infinity, so that one has to adopt a velocity cut-off in order to have a finite total volume. The cut-off has some influence in the results, however, because there are few particles with high velocities and, particularly for volume choice 1, these few particles are assigned large volumes (i.e. they weight heavily in equation 9). We experimented with 2, 2.5 and 3σ cut-offs, and finally adopted the 2.5σ level, which was the one that offered the best fitting between the analytical and numerical results.

The results for cases a, b and c are presented in Figs 1, 2 and 3, respectively, in which the amplitude of the wave relative to its initial value is plotted against the elapsed time. In each case, the theoretical prediction is shown as a solid line, the numerical results obtained with volume choice 1 are shown as a dotted line, and those obtained with volume choice 2 are shown as a dashed line.

The limiting case where the wavelength of the perturbation is equal to the Jeans wavelength (Fig. 1) is not very well suited for numerical experiments because, being a limiting case, truncation and rounding errors may easily move it into the unstable regime. Our results are probably affected by this phenomenon since, although agreeing very well with the theoretical values in the short run, they become unstable later on. Nevertheless, it is interesting to note the excellent agreement over the first few time units, which reveals a

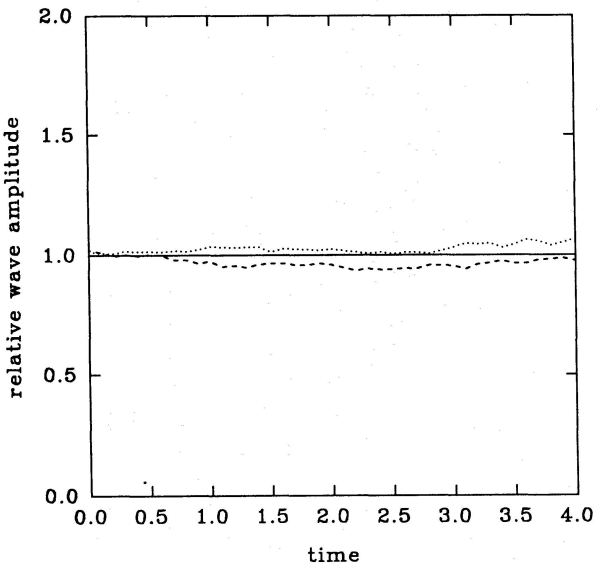

Figure 1. The amplitude of the wave, relative to its initial value, versus the elapsed time for case a (stationary wave). The theoretical values are shown as a solid line, and the numerical results as a dotted line (volume choice 1) and as a dashed line (volume choice 2).

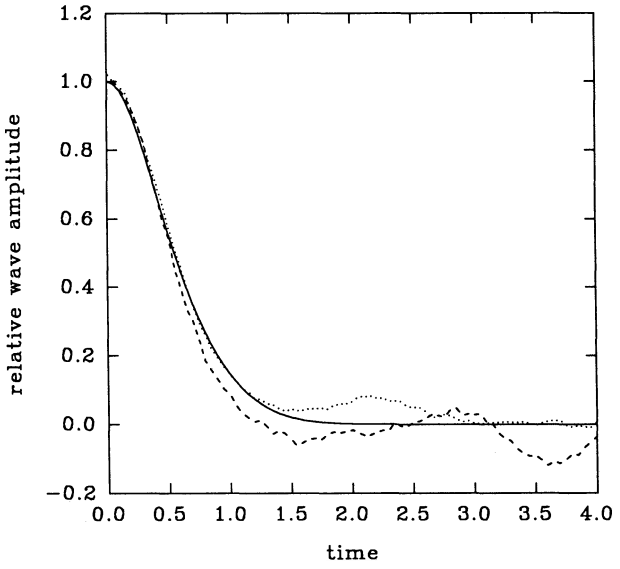

Figure 2. Same as Fig. 1, for case b (damped wave).

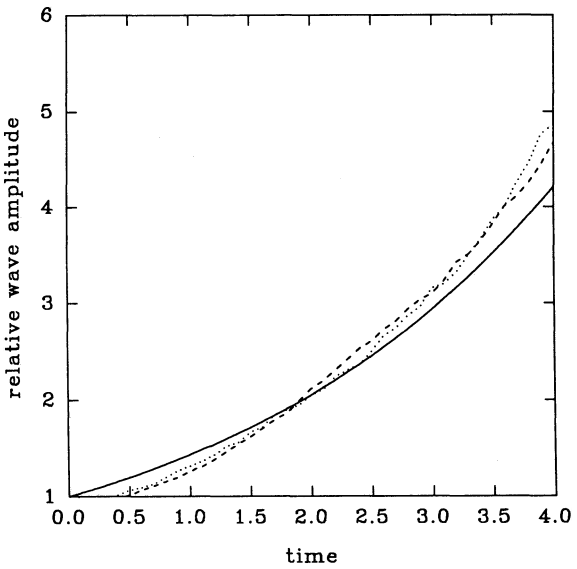

Figure 3. Same as Fig. 1, for case c (unstable wave).

stationary behaviour very different from that of the damped and unstable solutions of Figs 2 and 3, respectively, over the same time interval.

The similarly excellent agreement of the results shown in Fig. 2 is probably the result of the opposite effect: since the corresponding problem is actually damped, the physics of the process also contributes to the damping of any irregularities arising from the numerical process.

The intrinsic instability of example c may again be the cause of the departure of the numerical solutions from the theoretical solution after the first few time units. The agreement is reasonably good over the interval shown in the figure, which is remarkable considering that in this period the wave increased to more than 4 times its amplitude. One notes that, in an unstable system, any small error in the growth rate will eventually lead to arbitrarily large errors in the amplitudes.

It is worth noting that the results of Merritt (1987) for a different model tell essentially the same story: the agreement is excellent for the damped case, but both the stationary and the unstable cases show departures between theoretical and numerical results, which in the unstable case clearly increase with time.

As indicated in Section 3, the conservation of the total perturbation mass may be used to check the accuracy of the numerical solution. Fig. 4 presents a plot of the total perturbation mass against the elapsed time for volume choice 1, and Fig. 5 does the same for volume choice 2; in both figures, the results of examples a, b and c are represented, respectively, by dotted, solid and dashed lines. The initial total perturbation mass was zero, since we created a sinusoidal density distribution using both positive and negative masses for the perturbation particles; the total positive perturbation mass was, however, 0.025 initially, so this amount provides a reference value for the comparison.

The best behaviour is observed for the damped situation of case b, which conserved the total mass to within less than 0.34 per cent of the total positive mass throughout the computation for volume choice 1, and for which the result for volume choice 2, although not as good, is still within a very reasonable 1.3 per cent. Mass conservation is, on the other hand, much poorer for cases a and c: it might still be regarded as acceptable over the whole 4-unit interval considered for volume choice 1, but for volume choice 2 it exhibits unacceptably large fluctuations after about 3.0 and 1.5 time units, respectively, for cases a and c; departures exceeding 30 per cent are apparent for the strongly unstable case c. These gross departures are most probably linked to the physical instability of the problem in cases a and c, because they could not be avoided by reducing the time-step of the integration method; in fact, we got essentially the same results with half the time-step.

The conservation of the total perturbation mass might thus offer a way of checking for possible difficulties in the solution of a problem with this method; but the results of such a check must be treated with some caution. If we con-

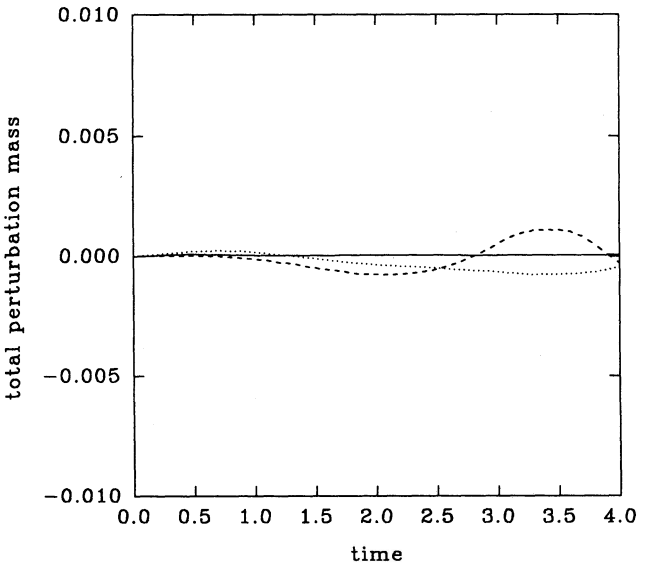

Figure 4. Total perturbation mass versus elapsed time for volume choice 1. The results for examples a, b and c are shown, respectively, as dotted, solid and dashed lines.

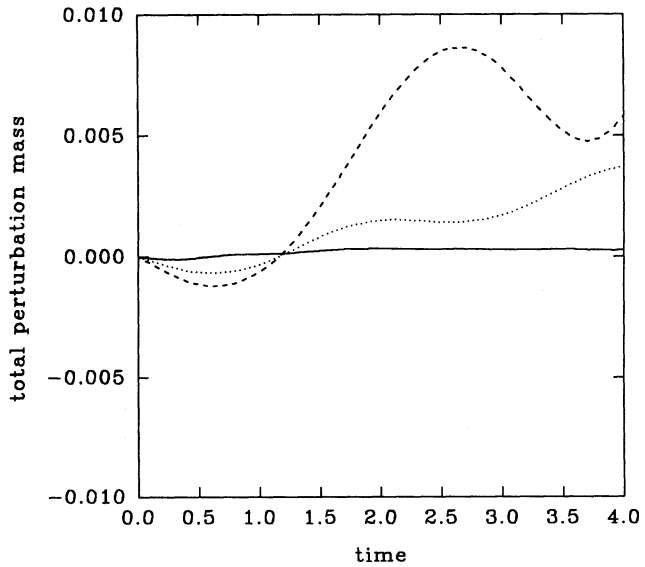

Figure 5. Same as Fig. 4, for volume 2.

sider the results obtained with the same volume choice, it is clear from Figs 4 and 5 that for poor total mass conservation the accuracy of the numerical results is also poor. This is not true, however, if we compare the results obtained with different volume choices: total mass is conserved much better with volume choice 1 than with volume choice 2; but the departures of the numerical results obtained with each volume choice from the analytical solutions are of the same order of magnitude.

5 DISCUSSION

The perturbation particle method seems to offer an efficient way of investigating the evolution of a perturbation in a stellar system in equilibrium. Since the particles are used to represent the perturbation only, no particles are wasted by being used to represent the (much more massive) equilibrium system.

The results are very good for stable systems. For unstable systems, the method is useful to reveal the instability, but it can only follow the evolution of an unstable perturbation for a relatively short time. This is only natural, and it is doubtful that any other method could do better.

As indicated above, the conservation of total perturbation mass offers a check of the results that should be treated with some care. Similarly to the case of energy conservation, one can be sure that the results are wrong when conservation is violated, but one cannot be sure that the results are right just because conservation is satisfied.

The results obtained with the two different choices of phase-space volume are very similar; this is particularly remarkable if we recall that the differences between the two volume choices are significant, as shown by Table 1. Thus we may conclude that the method is robust, in the sense that it is not particularly sensitive to the choice of the phase-space volumes. Nevertheless, the conservation of total perturbation mass, shown in Figs 4 and 5, suggests that choice 1 must be preferred: not only does it better conserve the total mass in the three cases, but it also gives cyclic total mass changes; while with choice 2 there is a systematic trend toward larger values. The good agreement of the results obtained with the two different volume choices should not make us forget that the method is indeed sensitive to the cut-offs demanded by the use of distribution functions that extend to infinity. With a 3σ rather than a 2.5σ cut-off, the total mass changes are almost 10 times larger with volume choice 1 and about double with choice 2; the agreement between analytical and numerical results is also somewhat poorer with the 3σ cut-off. Perhaps the most sensible attitude to adopt is that, while the method is indeed robust, one has to be alert to cases where a few individual particles may be assigned very large volumes.

Last, but not least, the simple theoretical model presented in Section 3 may be useful to check other methods for investigating the stability of stellar systems in equilibrium.

ACKNOWLEDGMENTS

We are very grateful to Daniel D. Carpintero, Pablo M. Cincotta, Angel R. Plastino and David Merritt for useful data and suggestions. The support through grants of the Fundación Antorchas and of the Consejo Nacional de Investigaciones Científicas y Técnicas de la República Argentina is gratefully acknowledged.

REFERENCES

Aarseth S. J., 1985, Multiple Time Scales. Academic Press, New York, p. 377
Binney J., Tremaine S., 1987, Galactic Dynamics. Princeton Univ. Press, Princeton, NJ
Hernquist L., Ostriker J. P., 1992, ApJ, 386, 375
Maoz E., 1991, ApJ, 375, 687
Merritt D., 1987, in de Zeeuw T., ed., IAU Symp. 127, Structure and Dynamics of Elliptical Galaxies. Reidel, Dordrecht, p. 315
Merritt D., Aguilar L. A., 1985, MNRAS, 217, 787